International Journal of Solids and Structures 50 (2013) 4217–4225

Contents lists available at ScienceDirect

International Journal of Solids and Structures

journal homepage: www.elsevier.com/locate/ijsolstr

Meshless methods for the inverse problem related to the determination of elastoplastic properties from the torsional experiment

Jan A. Kolodziej [1], Malgorzata A. Jankowska [2], Magdalena Mierzwiczak *

Poznan University of Technology, Institute of Applied Mechanics, Jana Pawla II 24, 60-965 Poznan, Poland

ARTICLE INFO

Article history:
Received 17 January 2013
Received in revised form 28 June 2013
Available online 5 September 2013

Keywords:
Method of fundamental solutions
Kansa method
Plane elastoplastic problem

ABSTRACT

The problem of determining the elastoplastic properties of a prismatic bar from the given experimental relation between the torsional moment M and the angle of twist per unit length of the rod's length θ is investigated as an inverse problem. The proposed method to solve the inverse problem is based on the solution of some sequences of the direct problem by applying the Levenberg-Marquardt iteration method. In the direct problem, these properties are known, and the torsional moment is calculated as a function of the angle of twist from the solution of a non-linear boundary value problem. This non-linear problem results from the Saint-Venant displacement assumption, the Ramberg–Osgood constitutive equation, and the deformation theory of plasticity for the stress–strain relation. To solve the direct problem in each iteration step, the Kansa method is used for the circular cross section of the rod, or the method of fundamental solutions (MFS) and the method of particular solutions (MPS) are used for the prismatic cross section of the rod. The non-linear torsion problem in the plastic region is solved using the Picard iteration.

1. Introduction

The torsion analysis of bars has a long history and can be traced back to Saint-Venant, who provided a final conclusion to the problem of elastic uniform torsion. The Saint-Venant semi-inverse method is used notably often for elastic and elastoplastic torsion analyses (see for example, the following texts: Chakrabarty, 1987, Chapter 3; Mendelson, 1968, Chapter 11; and Kliusznikov, 1979, Chapter 4). The main interest from a designer point of view is the torsional rigidity, which can be easily obtained from the relations between the torsional moment and the angle of twist per unit length. If the elastoplastic material properties of a bar are known, this relation is obtained by solving a non-linear boundary value problem. Here, such problem is called a direct problem of elastoplastic torsion.

Currently, there are many methods to solve a direct problem. Nadai (1931) was the first to propose a solution for an elastoplastic pure-torsion problem, and he calculated a fully plastic torque based on his sand heap analogy. In this analogy, sand is piled onto a horizontal table with the shape of the cross section of a bar. The slope of the resulting heap cannot exceed the angle of internal friction, which corresponds to the shear yield stress. Sadowsky (1941) extended this analogy to sections with holes. Nadai (1954) developed an approximate solution for an elastoplastic torsion by combining the membrane analogy and the sand heap analogy. The analytical solution for the elastoplastic problem was first proposed by Sokolovsky (1942); he prepared and used independent governing equations for elastic and plastic regions. He also developed a solution for the torsion of an oval section of a bar of an elastic/perfectly plastic material using an inverse method. Christopherson (1940) obtained a numerical solution for an elastoplastic problem for an I-section using the finite deference method (FDM) and the relaxation method. The analytical solutions of rectangular sections, which have elastoplastic material property, were developed by Smith and Sidebottom (1965) based on the Rayleigh–Ritz expansion and the principle of stationary complementary energy. Hodge (1966, 1967) used non-linear programming for the elastoplastic torsion problem for perfectly plastic material. Hodge et al. (1968) used the comparison between FDM and the non-linear programming method in solving elastoplastic torsion problems. Yamada et al. (1972) studied the elastoplastic uniform torsion and was the first to the finite element method (FEM). Baba and Kajita (1982) used a 2-node, 4-degree-of-freedom beam element for the uniform torsion analysis and a 4-node, 12-degree-of-freedom rect-

* Corresponding author. Address: Poznan University of Technology, Institute of Applied Mechanics, 24, Jana Pawla II Street, 60-965 Poznan, Poland. Tel.: +48 61 665 2387; fax: +48 61 665 2307.

E-mail addresses: jan.kolodziej@put.poznan.pl (J.A. Kolodziej), malgorzata.jankowska@put.poznan.pl, www.tm.am.put.poznan.pl (M.A. Jankowska), magdalena.mierzwiczak@wp.pl, magdalena.mierzwiczak@put.poznan.pl (M. Mierzwiczak).

URL: http://www.tm.am.put.poznan.pl.

[1] Tel.: +48 61 665 2321; fax: +48 61 665 2307.

[2] Tel.: +48 61 665 2069; fax: +48 61 665 2307.

0020-7683/$ - see front matter © 2013 Elsevier Ltd. All rights reserved.
http://dx.doi.org/10.1016/j.ijsolstr.2013.08.025

angular section element for the warping analysis of the sections. May and Al-Shaarbaf (1989) used a standard 3-dimensional, 20-node isoparametric quadratic brick element in the elastoplastic analysis of the uniform and non-uniform torsion of members that were subjected to pure and warping torsion. Dwivedi et al. (1990) used FDM to solve a torsional springback in a square bar with non-linear work-hardening material. The authors used the deformation theory of plasticity with a Ramber–Osgood-type stress–strain relationship. The problem of torsional springback was also considered (Dwivedi et al., 2002, 1992a, 1992b). Billinghurst et al. (1992) developed a miter model for the shear strain distribution in steel members under uniform torsion. Baniassadi et al. (2010) proposed a solution for the torsion of a heat-treated rod of an elastic/perfectly plastic material using a semi-inverse method. The method of fundamental solutions (MFS) for the elastoplastic torsion of prismatic rods has been presented (Kołodziej and Gorzelańczyk, 2012).If the elastoplastic material properties are not known and are determined from experimentally provided discrete values of the torsional moment $M_{Ti} = M_T(\theta_i)$ and the angle of twist per unit length θ_i, we have an inverse problem of elastoplastic torsion. Such inverse problem has received relatively less attention in literature than the direct problem. Mamedov (1995, 1998) considered the inverse problem to determine the so-called plasticity function in the Hencky correlation. The inverse problem was solved by solving the sequence direct problem using finite element method. In the study by Hasanov and Tatar (2010a), the plasticity function was also identified within the range of the J_2-deformation theory. The method used by the authors was based on the finite-difference discretization of the non-linear elastoplastic problem and on the parameterization of the unknown plasticity curve. Similar considerations were provided in by Hasanov and Tatar (2010b), where the authors considered a power-law material. In the aforementioned papers, the mesh methods (FEM and FDM) were used to solve the inverse elastoplastic problems. In recent decades, meshless methods have become popular in computational mechanics. For example, the MFS method was successfully used to solve inverse heat conduction problems. Currently, MFS is applied in the following inverse heat conduction problems, which involve the identification of heat sources (Mierzwiczak and Kołodziej, 2010; Yan et al., 2008, 2009; Kołodziej et al., 2010; Jin and Marin, 2007; Mierzwiczak and Kołodziej, 2011 and Yang et al., 2013), the boundary heat flux (Xiong et al., 2010; Hon and Wei, 2004; Dong et al., 2007; Shidfar et al., 2009), the Cauchy problem (Li et al., 2011; Yang and Ling, 2011; Marin, 2005; Wei et al., 2007; Zhou and Wei, 2008; Shigeta and Young, 2009; Marin, 2011; Wei et al., 2013), the backward heat conduction problem (Johansson et al., 2011a; Tsai et al. 2011), the Stefan problem (Johansson et al., 2011b) and the identification of the boundary geometry (Karageorghis and Lesnic, 2011; Lesnic and Bin-Mohsin, 2012; Bin-Mohsin and Lesnic, 2012). The aforementioned application of MFS is related to 2-dimensional problems. Another meshless method that can be used to solve 1-dimensional non-linear equations is the Kansa method (Kansa, 1990).

This paper aims to apply the MFS method to the inverse elastoplastic torsion problem in the prismatic rod case and to apply the Kansa method in the cylindrical rod case. There are many different models of isotropic elastoplasticity. Therefore, it is sometimes difficult to decide which model to use for a numerical implementation. In this paper, we chose the Ramberg–Osgood stress–strain relation (Huth, 1955). This model is advantageous because it does not have a well-defined yield point. Next, the torsion problem is simplified by the absence of a boundary between the elastic and plastic regions, which permits the same equations to apply throughout the cross section. To the best knowledge of the authors, this paper is the first application of this method to the inverse elastoplastic problem.

2. Problem formulation

The uniform torsion of prismatic rods may be formulated according to the deformation theory as follows

$$\frac{\partial}{\partial x}\left(\frac{1}{G}\cdot\frac{\partial\psi}{\partial x}\right)+\frac{\partial}{\partial y}\left(\frac{1}{G}\cdot\frac{\partial\psi}{\partial y}\right)=-2\theta \quad \text{in } \Omega_e, \tag{1}$$

where $\psi(x,y)$ is the Prandtl's stress function, θ is an angle of twist per unit length of the rod, G is a secant shear modulus, Ω_e is the cross sectional region of the bar.

The only two non-zero components of the stress tensor are given by

$$\sigma_{xz}=\frac{\partial\psi}{\partial y}, \quad \sigma_{yz}=-\frac{\partial\psi}{\partial x}. \tag{2}$$

The resultant shear stress is given by

$$\tau=\left[\left(\frac{\partial\psi}{\partial x}\right)^2+\left(\frac{\partial\psi}{\partial y}\right)^2\right]^{\frac{1}{2}}. \tag{3}$$

Because the lines of shear stress at each point of the section boundary must be directed along the tangent to the boundary, the lateral surface of the bar is stress-free, and the boundary curve Γ must be a line of constant stress function. For a simply connected cross section, we may take

$$\psi=0 \quad \text{on } \Gamma. \tag{4}$$

For the elastic torsion, the secant shear modulus is constant and is known as the elastic shear modulus. Consequently, in this region, the torsional rigidity is constant, and the torsional moment is linearly related to the angle of twist per unit length. For the elastoplastic torsion, there are a few different models of plastic behavior. Here, we will use the Ramberg–Osgood for the secant shear modulus in the following form

$$\frac{1}{G}=\frac{1}{G_0}\left[1+\frac{\beta}{G_0^n}\left\{\left(\frac{\partial\psi}{\partial x}\right)^2+\left(\frac{\partial\psi}{\partial y}\right)^2\right\}^{\frac{n}{2}}\right], \tag{5}$$

where G_0 is the elastic shear modulus, and β and n are dimensionless constants that characterize the given material.

Putting (5) into (1), we have the following governing equation

$$\frac{\partial}{\partial x}\left\{\left[1+\frac{\beta}{G_0^n}\left(\left(\frac{\partial\psi}{\partial x}\right)^2+\left(\frac{\partial\psi}{\partial y}\right)^2\right)^{\frac{n}{2}}\right]\frac{\partial\psi}{\partial x}\right\} + \frac{\partial}{\partial y}\left\{\left[1+\frac{\beta}{G_0^n}\left(\left(\frac{\partial\psi}{\partial x}\right)^2+\left(\frac{\partial\psi}{\partial y}\right)^2\right)^{\frac{n}{2}}\right]\frac{\partial\psi}{\partial y}\right\}=-2\theta\cdot G_0. \tag{6}$$

The torsional moment can readily be obtained by integrating the stress function

$$M_T=2\iint_\Omega \psi\,dxdy. \tag{7}$$

It is convenient to introduce the following dimensionless quantities

$$\Psi=\frac{\psi}{a\cdot\tau_p}, \quad X=\frac{x}{a}, \quad Y=\frac{y}{a}, \quad \tilde{\theta}=\frac{\theta\cdot G_0\cdot a}{\tau_p}, \quad \kappa=\frac{\beta\cdot\tau_p^n}{G_0^n}, \quad \tilde{M}_T=\frac{M_T}{a^3\cdot\tau_p}, \tag{8}$$

where a is a characteristic dimension of the cross section, and τ_p is a nominal yield stress.

Then, the governing equation and the boundary condition have the following forms

$$\nabla^2\Psi = -\frac{1}{1+\kappa\cdot T^n}\left\{2\tilde{\theta}+\kappa\cdot n\cdot T^{n-2}\left[\left(\frac{\partial\Psi}{\partial X}\right)^2\frac{\partial^2\Psi}{\partial X^2}+2\frac{\partial\Psi}{\partial X}\frac{\partial\Psi}{\partial Y}\frac{\partial^2\Psi}{\partial X\partial Y}+\left(\frac{\partial\Psi}{\partial Y}\right)^2\frac{\partial^2\Psi}{\partial Y^2}\right]\right\} \quad \text{in } \Omega_e, \tag{9}$$

$$\Psi = 0 \quad \text{on } \Gamma, \tag{10}$$

where T is the non-dimensional resultant shear stress given as follows

$$T = \frac{1}{\tau_p}\left[\left(\frac{\partial\psi}{\partial x}\right)^2+\left(\frac{\partial\psi}{\partial y}\right)^2\right]^{\frac{1}{2}} = \left[\left(\frac{\partial\Psi}{\partial X}\right)^2+\left(\frac{\partial\Psi}{\partial Y}\right)^2\right]^{\frac{1}{2}}. \tag{11}$$

The non-dimensional torsional moment has the form

$$\tilde{M}_T = 2\iint_{\Omega_e}\Psi\cdot dXdY. \tag{12}$$

For the torsion of the rod with a circular cross section, the stress function is only a function of polar coordinates, and Eq. (1) takes the form

$$\frac{1}{r}\frac{d}{dr}\left(\frac{r}{G}\cdot\frac{d\psi}{dr}\right) = -2\theta, \quad 0\leqslant r\leqslant a, \tag{13}$$

where a is the radius of the rod, and the secant shear modulus is given by

$$\frac{1}{G} = \frac{1}{G_0}\left[1+\frac{\beta}{G_0^n}\left|\frac{d\psi}{dr}\right|^n\right]. \tag{14}$$

The shear stress is given by

$$\tau = \frac{d\psi}{dr}. \tag{15}$$

Eq. (13) must be solved with the following boundary conditions

$$\psi = 0 \quad \text{for } r = a, \qquad \frac{d\psi}{dr} = 0 \quad \text{for } r = 0. \qquad rm16)$$

After introducing the non-dimensional variables (8) and $R = r/a$, Eq. (13) and the boundary conditions (16) take the forms

$$\left(1+\kappa\cdot\left|\frac{d\Psi}{dR}\right|^n\right)\left(\frac{d^2\Psi}{dR^2}+\frac{1}{R}\frac{d\Psi}{dR}\right) = -2\tilde{\theta}-\kappa\cdot n\cdot\left|\frac{d\Psi}{dR}\right|^n\frac{d^2\Psi}{dR^2} \quad \text{in } \Omega_e, \tag{17}$$

$$\Psi = 0 \quad \text{for } R = 1, \qquad \frac{d\Psi}{dR} = 0 \quad \text{for } R = 0. \tag{18}$$

The non-dimensional torsional moment has the form

$$\tilde{M}_T = 4\pi\int_0^1\Psi R dR. \tag{19}$$

The direct elastoplastic problem depends on solving Eq. (9) with boundary condition (10) for the square cross section of the rod or Eq. (17) with boundary condition (18) for the circular cross section of the rod. In such cases, the non-dimensional angle of twist $\tilde{\theta}$ and the non-dimensional material parameters κ and n are known. After determining the stress function Ψ, the torsional moment is calculated. As mentioned above, the purpose of this paper is to apply the MFS to solve the inverse elastoplastic problem. The proposed method is based on the Leveberg-Marquadt iteration, which requires solving the direct problems at each iteration step.

3. Application of meshless methods to solve direct and inverse problems

In the direct problem, the non-dimensional angle of twist $\tilde{\theta}$ and the non-dimensional material parameters κ and n are known. The problem lies in solving the non-linear differential equation (9) with boundary condition (10) or Eq. (17) with boundary condition (18) for the square or the cylindrical cross section of the rod, respectively.

Algorithm 1 – direct problem for the square cross section of the rod

Step 1. Choose the initial values for the parameters $\kappa = 0$ and $n = 0$.

Take $j = 0$ and solve a simple problem using the MFS method

$$\nabla^2\Psi_j = -2\tilde{\theta}, \quad (X,Y)\in\Omega,$$

$$\Psi_j(X,Y) = 0, \quad (X,Y)\in\Gamma_1,$$

$$\frac{\partial\Psi_j(X,Y)}{\partial n} = 0, \quad (X,Y)\in\Gamma_2,$$

$$\Psi_j(X,Y) = \sum_{i=1}^{Ns}c_i\ln\left(\sqrt{(X-X_i)^2+(Y-Y_i)^2}\right)-\frac{\tilde{\theta}}{2}(X^2+Y^2). \tag{20}$$

Remark. In the numerical experiment, the cross section of the bars can have an axis of symmetry. In such cases, it is convenient to consider some repeated elements of the cross section. On the axis of symmetry Γ_2 in the repeated element, one has the boundary condition with a normal derivative, and the other parts of the boundary Γ_1, have the Dirichlet boundary conditions.

Step 2. For known κ, n values, the right-hand-side function can be approximated as

$$f(X,Y) = -\frac{1}{1+\kappa\cdot T_j^n}\left\{2\tilde{\theta}+\kappa\cdot n\cdot T_j^{n-2}\left[\left(\frac{\partial\Psi_j}{\partial X}\right)^2\frac{\partial^2\Psi_j}{\partial X^2}+2\frac{\partial\Psi_j}{\partial X}\frac{\partial\Psi_j}{\partial Y}\frac{\partial^2\Psi_j}{\partial X\partial Y}+\left(\frac{\partial\Psi_j}{\partial Y}\right)^2\frac{\partial^2\Psi_j}{\partial Y^2}\right]\right\},$$

using the radial basis function and the monomials

$$f(X,Y)\cong\sum_{m=1}^{Ni}\alpha_m\hat{\varphi}(\hat{R}_m)+\sum_{k=1}^{K}\beta_k\tilde{\varphi}_k(X,Y), \tag{21}$$

where $\hat{R}_m = \sqrt{(X-X_m)^2+(Y-Y_m)^2}$

$$\sum_{m=1}^{Ni}\alpha_m\hat{\varphi}(\hat{R}_{lm})+\sum_{k=1}^{K}\beta_k\tilde{\varphi}_k(X_l,Y_l) = \tilde{f}(X_l,Y_l), \quad l = 1,2,\ldots,Ni,$$

$$\sum_{m=1}^{Ni}\alpha_m\tilde{\varphi}_k(X_m,Y_m) = 0, \quad k = 1,2,\ldots,K.$$

Step 3. Calculate the particular solution

$$\Psi_{j+1}^p(X,Y) = \sum_{m=1}^{Ni}\alpha_m^{(j+1)}\hat{\psi}(\hat{R}_m)+\sum_{k=1}^{K}\beta_k^{(j+1)}\tilde{\psi}_k(X,Y). \tag{22}$$

Step 4. Solve the homogenous problem

$$\nabla^2\Psi_{j+1}^h(X,Y) = 0, \quad (X,Y)\in\Omega,$$

$$\Psi_{j+1}^h(X,Y) = -\Psi_{j+1}^p(X,Y), \quad (X,Y)\in\Gamma_1,$$

$$\frac{\partial\Psi_{j+1}^h(X,Y)}{\partial n} = -\frac{\partial\Psi_{j+1}^p(X,Y)}{\partial n}, \quad (X,Y)\in\Gamma_2$$

using the MFS method.

Step 5. Calculate the solution as a sum of the homogenous and the particular solutions

$$\Psi_{j+1}(X,Y) = \sum_{i=1}^{Ns} c_i^{(j+1)} \ln\left(\sqrt{(X-X_i)^2 + (Y-Y_i)^2}\right) + \sum_{m=1}^{Ni} \alpha_m^{(j+1)} \hat{\psi}(\hat{R}_m) + \sum_{k=1}^{K} \beta_k^{(j+1)} \tilde{\psi}_k(X,Y). \tag{23}$$

Step 6. Evaluate $\varepsilon_\Psi = \|\Psi_{j+1} - \Psi_j\|_2$.

If $\varepsilon_\Psi \leqslant tol$, calculate $\tilde{M}_T(\tilde{\theta},\kappa,n) = 2\int\int_{\tilde{\Omega}_e} \Psi_{j+1} \cdot dXdY$ and STOP.

Else, take $j = j + 1$ and go back to Step 2.

Algorithm 2 – direct problem for the circular cross section of the rod

Step 1. Choose the initial values for the parameters $\kappa = 0$, $n = 0$.

Take $j = 0$ and solve the simple problem

$$\frac{d^2\Psi_0}{dR^2} + \frac{1}{R}\frac{d\Psi_0}{dR} = -2\tilde{\theta},$$

$$\Psi_0 = 0 \quad \text{for } R = 1,$$

$$\frac{d\Psi_0}{dR} = 0 \quad \text{for } R = 0,$$

$$\Psi_0 = \frac{\tilde{\theta}}{2}(1 - R^2).$$

Step 2. Make a uniform distribution of the area with N nodes $R_i = (i-1)/(N-1)$, $i = 1, 2, \ldots, N$.

Step 3. For known κ, n, take $j = j + 1$ and solve the linear boundary value problem

$$\frac{d^2\Psi_j}{dR^2} + \frac{1}{R}\frac{d\Psi_j}{dR} = -\left\{2\tilde{\theta} + \kappa \cdot n \cdot \left|\frac{d\Psi_{j-1}}{dR}\right|^n \frac{d^2\Psi_{j-1}}{dR^2}\right\}\left(1 + \kappa \cdot \left|\frac{d\Psi_{j-1}}{dR}\right|^n\right)^{-1},$$

$$\Psi_j = 0, \quad R = 1,$$

$$\frac{d\Psi_j}{dR} = 0, \quad R = 0$$

using the Kansa collocation method.

Step 4. Calculate the solution as a linear combination of the multiquadric functions

$$\Psi_j = \sum_{i=1}^{N} c_i^{(j)} \sqrt{(R - R_i)^2 + c^2},$$

where c is the shape parameter.

Step 5. Evaluate $\varepsilon_\Psi = \|\Psi_{j+1} - \Psi_j\|_2$.

If $\varepsilon_\Psi \leqslant tol$, calculate $\tilde{M}_T = 4\pi\int_0^1 \Psi R dR$ and STOP.

Else, go back to Step 3.

In the inverse problem, the non-dimensional material parameters κ and n are unknown, but we know the non-dimensional torsional moment as a function of the non-dimensional angle of twist $\tilde{M}_T = \tilde{M}_T(\tilde{\theta})$. To solve this problem for both the prismatic and the cylindrical cross sections of the rod, the Levenberg–Marquardt method can be used according to the following algorithm (Press et al., 1992).

Algorithm 3 – inverse problem for the square and the circular cross sections

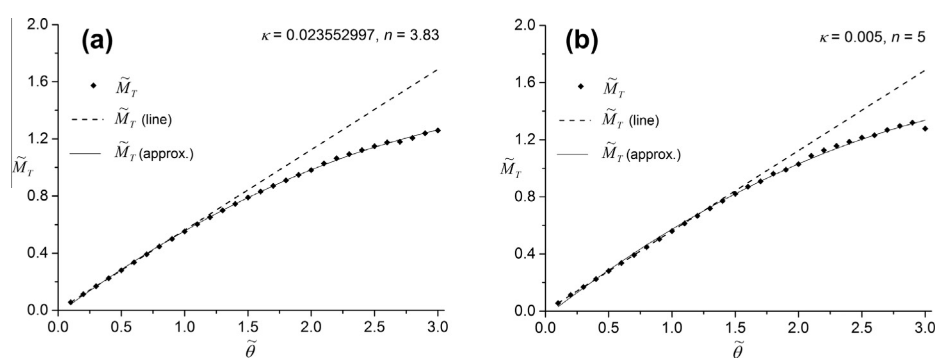

Fig. 1. The non-dimensional torsional moment $\tilde{M}_T$ as a function of the non-dimensional angle of twist $\tilde{\theta}$ for the square cross section of the rod and for two different values of parameters κ, n.

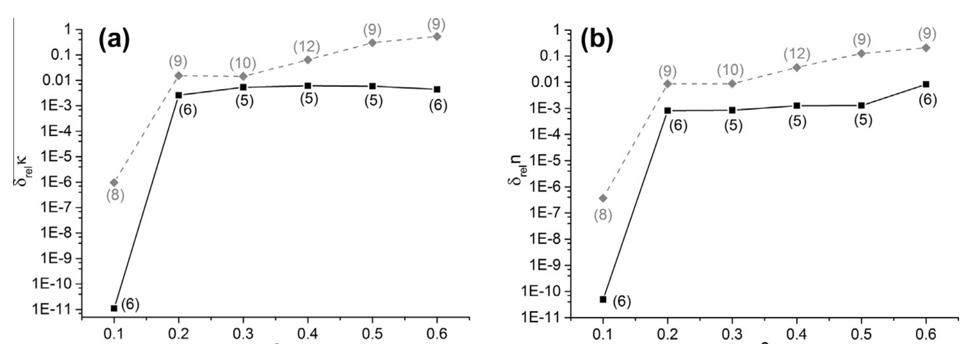

Fig. 2. The influence of the multi-quadric parameter c on the accuracy of the approximate solution in the lower (black solid line) and upper (gray dashed line) range of $\tilde{\theta}$ together with the number of Levenberg–Marquardt iterations (in brackets) ($Ns = Nc = 80$, $Ni = 100$, $s = 0.2$ and $\kappa_0 = 0.021195$, $n_0 = 3.447$).

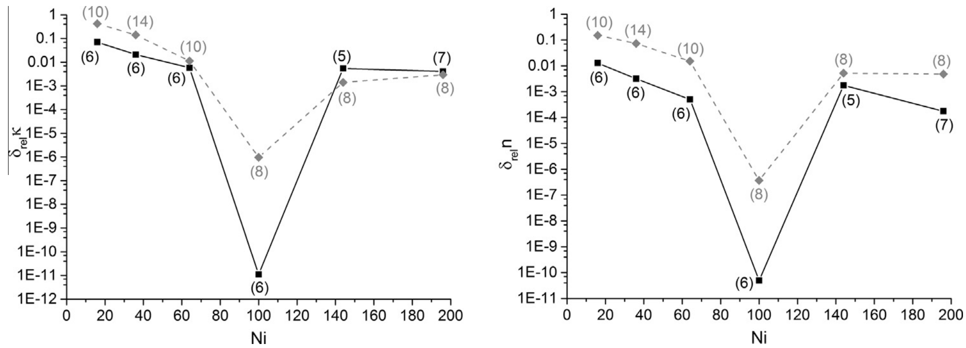

Fig. 3. The influence of the number *Ni* of the RBF functions on the accuracy of the approximate solution in the lower (black solid line) and upper (gray dashed line) range of $\tilde{\theta}$ together with the number of Levenberg–Marquardt iterations (in brackets) ($Ns = Nc = 80$, $c = 0.1$, $s = 0.2$ and $\kappa_0 = 0.021195$, $n_0 = 3.447$).

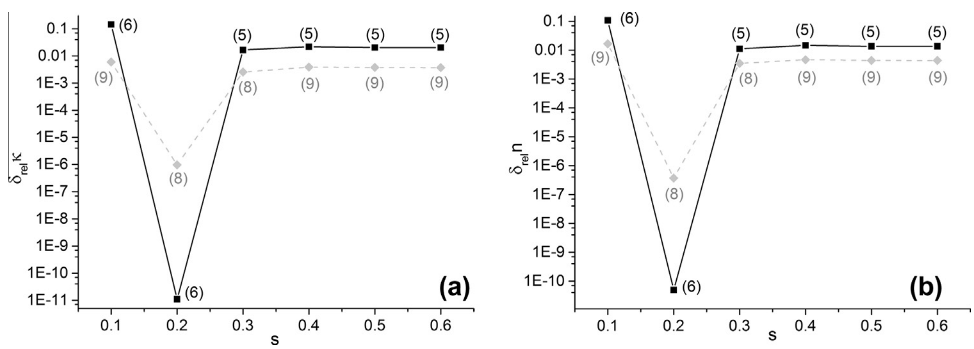

Fig. 4. The influence of the distance *s* of the source points to the fictitious boundary on the accuracy of the approximate solution in the lower (black solid line) and upper (gray dashed line) range of $\tilde{\theta}$ together with the number of Levenberg–Marquardt iterations (in brackets) ($Ns = Nc = 80$, $Ni = 100$, $c = 0.1$ and $\kappa_0 = 0.021195$, $n_0 = 3.447$).

Step 1. Choose an initial guess for the fitted parameters $\kappa = \kappa_0$, $n = n_0$ and the constants h_κ, h_n subsequently used for the approximation of derivatives with the central finite differences.

Step 2. Compute $\varepsilon(\kappa, n)$ according to the following formula

$$\varepsilon(\kappa, n) = \sum_{i=1}^{Ne} \left[\tilde{M}_T(\tilde{\theta}_i, \kappa, n) - \tilde{M}_{Ti}\right]^2, \tag{24}$$

$$\frac{\partial \varepsilon(\kappa, n)}{\partial \kappa} = 2\sum_{i=1}^{Ne} [\tilde{M}_T(\tilde{\theta}_i, \kappa, n) - \tilde{M}_{Ti}] \times \frac{\tilde{M}_T(\tilde{\theta}_i, \kappa + h_\kappa, n) - \tilde{M}_T(\tilde{\theta}_i, \kappa - h_\kappa, n)}{2 \cdot h_\kappa},$$

$$\frac{\partial \varepsilon(\kappa, n)}{\partial n} = 2\sum_{i=1}^{Ne} [\tilde{M}_T(\tilde{\theta}_i, \kappa, n) - \tilde{M}_{Ti}] \times \frac{\tilde{M}_T(\tilde{\theta}_i, \kappa, n + h_n) - \tilde{M}_T(\tilde{\theta}_i, \kappa, n - h_n)}{2 \cdot h_n}.$$

Remark. This step requires solving the *direct problem* (Algorithm 1 or 2) $5 \cdot N_e$ times.

Step 3. Pick a modest value for λ, e.g. $\lambda = 0.001$.

Step 4. Solve the linear system of equations

$$\begin{bmatrix} A_{1,1} & A_{1,2} \\ A_{2,1} & A_{2,2} \end{bmatrix} \begin{bmatrix} \delta\kappa \\ \delta n \end{bmatrix} = \begin{bmatrix} b_1 \\ b_2 \end{bmatrix}, \tag{25}$$

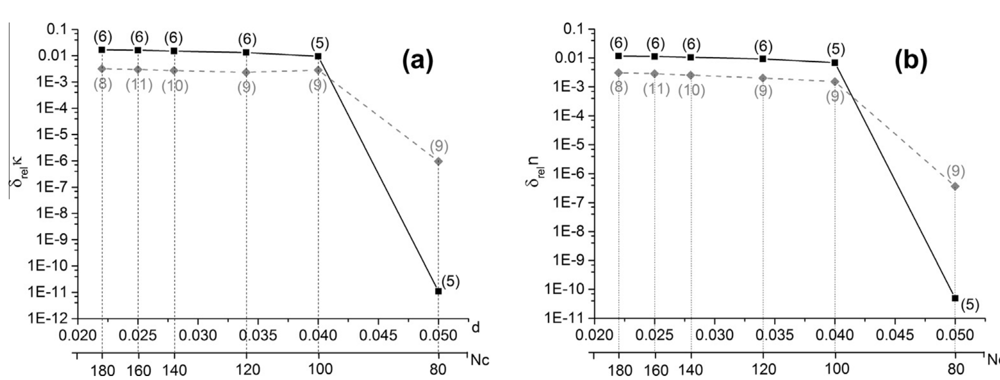

Fig. 5. The influence of the distance *d* between the collocation points on the accuracy of the approximate solution in the lower (black solid line) and upper (gray dashed line) range of $\tilde{\theta}$ together with the number of Levenberg–Marquardt iterations (in brackets) ($Ns = 80$, $Ni = 100$, $c = 0.1$, $s = 0.2$ and $\kappa_0 = 0.021195$, $n_0 = 3.447$).

Table 1
The identification of the material parameters (κ = 0.023552997, n = 3.83) for a square cross section of the rod in the lower range of $\tilde{\theta}$ for different number Ne of data points and selected initial values κ_0, n_0. ($Ns = Nc$ = 80, Ni = 100, c = 0.1, s = 0.2).

Ne	Iteration	κ	n	$\delta_{rel}\kappa$	$\delta_{rel}n$
κ_0 = 0.0223725, n_0 = 3.6385					
15	5	0.0235529972	3.8299999992	4.25E−11	1.92E−10
30	5	0.0235529972	3.8299999999	8.20E−11	4.33E−12
60	5	0.0235529972	3.8299999999	4.00E−12	9.34E−13
κ_0 = 0.021195, n_0 = 3.447					
15	6	0.0235529972	3.8300000001	1.10E−11	4.95E−11
30	6	0.0235529972	3.8300000000	1.19E−11	6.29E−13
60	6	0.0235529972	3.8300000000	2.56E−13	5.98E−14
κ_0 = 0.0200175, n_0 = 3.2555					
15	6	0.0235529972	3.8300000004	2.79E−11	1.26E−10
30	6	0.0235529972	3.8299999999	5.98E−12	3.15E−13
60	6	0.0235529972	3.8299999999	1.58E−13	3.61E−14
κ_0 = 0.01884, n_0 = 3.064					
15	6	0.0235529972	3.8299999993	3.84E−11	1.73E−10
30	6	0.0235529972	3.8299999999	5.51E−11	2.91E−12
60	7	0.0235529972	3.8299999999	1.16E−13	2.69E−14

Table 2
The identification of the material parameters (κ = 0.023552997, n = 3.83) for a square cross section of the rod in the upper range of $\tilde{\theta}$ for different number Ne of data points and selected initial values κ_0, n_0 ($Ns = Nc$ = 80, Ni = 100, c = 0.1, s = 0.2).

Ne	Iteration	κ	n	$\delta_{rel}\kappa$	$\delta_{rel}n$
κ_0 = 0.0223725, n_0 = 3.6385					
15	8	0.0235530263	3.8299982061	1.23E−06	4.68E−07
30	9	0.0235529952	3.8300001224	8.27E−08	3.02E−08
60	10	0.0235530037	3.8299996387	2.76E−07	9.43E−08
κ_0 = 0.021195, n_0 = 3.447					
15	8	0.0235530199	3.8299985964	9.67E−07	3.67E−07
30	10	0.0235529950	3.8300001329	8.98E−08	3.47E−08
60	10	0.0235530037	3.8299996383	2.77E−07	9.44E−08
κ_0 = 0.0200175, n_0 = 3.2555					
15	8	0.0235530270	3.8299981632	1.26E−06	4.79E−07
30	8	0.0235529950	3.8300001345	9.10E−08	3.51E−08
60	10	0.0235529918	3.8300002949	2.25E−07	7.70E−08
κ_0 = 0.01884, n_0 = 3.064					
15	7	0.0235530084	3.8299993086	4.76E−07	1.80E−07
30	10	0.0235529934	3.8300002340	1.58E−07	6.11E−08
60	10	0.0235529806	3.8300009191	7.03E−07	2.49E−07

where $b_1 = -\frac{\partial\varepsilon}{\partial\kappa}$, $b_2 = -\frac{\partial\varepsilon}{\partial n}$, $A_{1,1} = (1+\lambda)\left(\frac{\partial\varepsilon}{\partial\kappa}\right)^2$, $A_{1,2} = A_{2,1} = \frac{\partial\varepsilon}{\partial\kappa}\frac{\partial\varepsilon}{\partial n}$, and $A_{2,2} = (1+\lambda)\left(\frac{\partial\varepsilon}{\partial n}\right)^2$.

Step 5. Evaluate $\varepsilon(\kappa+\delta\kappa, n+\delta n)$ (solve the direct problem – Algorithm 1 or 2 – N_e times).

Step 6. If $\varepsilon(\kappa+\delta\kappa, n+\delta n) \geqslant \varepsilon(\kappa, n)$, $\lambda = 10\cdot\lambda$ and go to Step 4.

Step 7. If $\varepsilon(\kappa+\delta\kappa, n+\delta n) < \varepsilon(\kappa, n)$, $\lambda = \lambda/10$, update the trial solution $\kappa = \kappa+\delta\kappa$, $n = n+\delta n$.

If $\|[\delta\kappa, \delta n]\|_2 \leqslant tol$, STOP; Else, go back to Step 4.

Note that in the above algorithms we use the following notation: Ns is the number of source points, Ni is the number of interpolation points $(X_l, Y_l) \in \Omega$ and K is the number of monomials. Subsequently, we denote by Nc the number of collocation points $(X_c, Y_c) \in \Gamma$, Subsequently, we denote by Nc the number of collocation points $(X_c, Y_c)\Gamma$. The source points are located on the fictitious contour similar to the boundary of the area at a given distance s. To interpolate the right hand side of the governing equations with the radial basis functions (RBF), the multiquadric function $\hat{\varphi}(\hat{R}_m) = \sqrt{\hat{R}_m^2 + c^2}$ is used with the shape factor c.

4. Numerical results

The first numerical experiment performed by the authors concerns a prismatic rod made of chrome-nickel steel, which is hard and is represented by the following G_0 = 65.16 MPa, $\beta = 2.1\cdot 10^7$, τ_p = 300 MPa, n = 3.83, and κ = 0.023552997 (Fig. 1(a)). In the second numerical experiment, we choose the material with the following parameter values n = 5, and κ = 0.005 (Fig. 1(b)). Subsequently, we analyze the properties of the methods proposed in the paper on the basis of the numerical results obtained for chrome-nickel steel.

Consider the prismatic rod with the square cross section. For the given parameters κ, n, the non-dimensional torsional moment $\tilde{M}_T = \tilde{M}_T(\tilde{\theta})$ is first approximated as a function of the non-dimensional angle of twist $\tilde{\theta}$ using Algorithm 1 (see also Fig. 1(a)). The obtained results $\{\tilde{M}_{T_i}, \tilde{\theta}_i\}_{i=1}^{Ne}$, where Ne denotes the number of data points, are used as input data for the inverse problem to determine the non-dimensional material parameters κ and n with Algorithm 3. For subsequent values of κ and n, in step 2 of Algorithm 3, the value of $\tilde{M}_T(\tilde{\theta}_i, \kappa, n)$ in (24) is calculated with Algorithm 1. The derivatives $\frac{\partial\tilde{M}_T(\tilde{\theta}_i,\kappa,n)}{\partial\kappa}$, $\frac{\partial\tilde{M}_T(\tilde{\theta}_i,\kappa,n)}{\partial n}$ are approximated with the central finite differences for h_κ = 0.001 and h_n = 0.005. For the comparison reasons we consider two different sets of the data points $\{\tilde{M}_{T_i}, \tilde{\theta}_i\}_{i=1}^{Ne}$ corresponding to two appropriate ranges of the angle of twist $\tilde{\theta}$. The first one (hereinafter referred to as the lower range) relates to $\tilde{\theta} \in (0, 1.5]$ and it features a nearly linear relationship between the angle of twist and the torsional moment. The second one (referred to as the upper range) relates to $\tilde{\theta} \in (1.0, 2.5]$ and it features a nonlinear characteristics (see also Fig. 1(a)). The material parameters κ and n are identified in each range considered for $Ne = \{15, 30, 60\}$, respectively.

First we study the influence of the MFS and MPS parameters on the accuracy of the numerical solutions. We choose a representa-

Table 3
The influence of the random noise of data points on the identification of the material parameters (κ = 0.023552997, n = 3.83) for a square cross section of the rod in the lower range of $\tilde{\theta}$ ($Ns = Nc$ = 80, Ni = 100, c = 0.1, s = 0.2 and κ_0 = 0.021195, n_0 = 3.447).

$\Delta\tilde{M}_T$ [%]	Iteration	κ	n	$\delta_{rel}\kappa$	$\delta_{rel}n$
0	6	0.0235529972	3.8300000001	1.09E−11	4.95E−11
0.25	5	0.0243347526	3.6619368209	3.32E−02	4.38E−02
0.5	7	0.0243241881	3.9032391855	3.27E−02	1.91E−02
0.75	7	0.0433559380	3.7810176098	3.32E−02	1.28E−02
1	5	0.0246830888	3.6347518964	4.80E−02	5.10E−02
1.25	7	0.0239005561	4.0024509887	1.47E−02	4.50E−02
1.5	6	0.0312134311	2.9570840882	3.25E−01	2.28E−01
1.75	6	0.0273350200	2.7837007061	1.60E−01	2.73E−01
2	5	0.0229706041	3.7156977987	2.47E−02	2.98E−02

Table 4
The influence of the random noise of data points on the identification of the material parameters (κ = 0.023552997, n = 3.83) for a square cross section of the rod in the upper range of $\tilde{\theta}$ ($Ns = Nc$ = 80, Ni = 100, c = 0.1, s = 0.2 and κ_0 = 0.021195, n_0 = 3.447).

$\Delta\tilde{M}_T$ [%]	Iteration	κ	n	$\delta_{rel}\kappa$	$\delta_{rel}n$
0	8	0.0235530199	3.8299985964	9.56E−07	3.67E−07
0.25	7	0.0243981939	3.7863549045	3.59E−02	1.14E−02
0.5	8	0.0243106205	3.7934715001	3.22E−02	9.54E−03
0.75	9	0.0234744667	3.8316327831	3.33E−03	4.26E−04
1	7	0.0222418407	3.8799870383	5.57E−02	1.31E−02
1.25	7	0.0243811410	3.7557077194	3.52E−02	1.94E−02
1.5	7	0.0248451388	3.7293421910	5.49E−02	2.63E−02
1.75	7	0.0248699252	3.7720064155	5.59E−02	1.51E−02
2	8	0.0242319343	3.8125008352	2.88E−02	4.57E−03

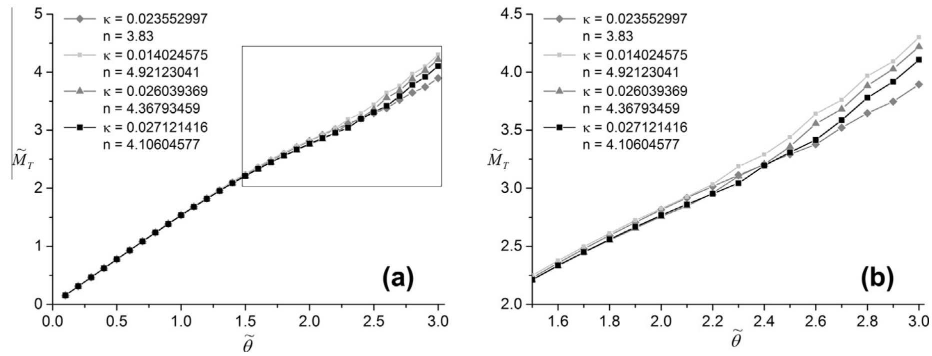

Fig. 6. The non-dimensional torsional moment $\tilde{M}_T$ as a function of the non-dimensional angle of twist $\tilde{\theta}$ for the cylindrical cross section of the rod for four different values of parameters κ, n.

Table 5
The identification of the material parameters (κ = 0.023552997, n = 3.83) for a for a cylindrical cross section of the rod for different number *Ne* of data and selected initial values κ_0, n_0 (N = 21, c = 0.1).

Ne	Iteration	κ	n	$\delta_{rel}\kappa$	$\delta_{rel}n$
κ_0 = 0.0223725, n_0 = 3.6385					
15	5	0.023580302	3.83102365	1.16E−03	2.67E−04
30	9	0.023573018	3.83100515	8.50E−04	2.62E−04
45	12	0.023560753	3.829379	3.29E−04	1.62E−04
60	12	0.023558322	3.83073284	2.26E−04	1.91E−04
κ_0 = 0.1, n_0 = 3.447					
15	5	0.023580357	3.83033308	1.16E−03	8.70E−05
30	6	0.023552997	3.83	1.16E−10	1.42E−13
45	8	0.023584659	3.82974971	1.34E−03	6.53E−05
60	10	0.023552997	3.83	1.00E−11	2.10E−11
κ_0 = 0.1, n_0 = 3.0					
15	9	0.033593588	3.00198089	4.26E−01	2.16E−01
30	29	0.034471288	2.93922104	4.64E−01	2.33E−01
45	18	0.033568516	2.98523579	4.25E−01	2.21E−01
60	6	0.034853126	2.91302017	4.80E−01	2.39E−01
κ_0 = 0.01, n_0 = 4.0					
15	27	0.023552997	3.83000002	1.34E−08	3.96E−09
30	11	0.023533189	3.83210575	8.41E−04	5.50E−04
45	26	0.023497404	3.83284157	2.36E−03	7.42E−04
60	32	0.023552996	3.83000003	3.30E−08	7.13E−09
κ_0 = 0.01, n_0 = 5.0					
15	22	0.023552997	3.83000002	1.69E−08	5.42E−09
30	25	0.023552997	3.83000002	1.73E−08	4.38E−09
45	28	0.023552997	3.83000002	2.15E−08	5.49E−09
60	32	0.023552997	3.83000002	2.40E−08	5.02E−09

tive set of values for the following parameters: the multi-quadric parameter c ($c = 0.1, 0.2, \ldots, 0.6$), the number *Ni* of the radial basis functions (RBF) that is equal to the number of interpolation points *Ni* (*Ni* = 16, 36, 64, 100, 144, 196), the distance s of the source points to the boundary ($s = 0.1, 0.2, \ldots, 0.6$) and the distance d between the collocation points (d = 0.05, 0.04, 0.034, 0.028, 0.025, 0.022) related to the appropriate number of collocation points *Nc* (*Nc* = 80, 100, 120, 140, 160, 180). We examine the numerical stability of the method considered with respect to the decreasing amount of noise added to the data. For this purpose we use the input data with some random disturbance value, i.e. we take

$$\tilde{\tilde{M}}_{T_i} = \tilde{M}_{T_i}(1 + RN \cdot \Delta\tilde{M}_T), \tag{26}$$

where $\Delta\tilde{M}_T \in [0, 2]$ (in%) is a disturbance's coefficient, $RN \in [-1, 1]$ is a random number, and $\tilde{\tilde{M}}_{T_i}$, $\tilde{M}_{T_i}$ are the disturbed and the exact the non-dimensional torsional moments, respectively. Then, we also choose four various pairs of the initial values $\{\kappa_0, n_0\}$ for the Levenberg–Marquardt method, i.e. $\{\kappa_0 = 0.0223725,\ n_0 = 3.6385\}$, $\{\kappa_0 = 0.021195,\ n_0 = 3.447\}$, $\{\kappa_0 = 0.0200175,\ n_0 = 3.2555\}$, $\{\kappa_0 = 0.01884,\ n_0 = 3.064\}$. Finally, with the exact values of κ and n known for the elastoplastic problem considered, the accuracy of the material parameters obtained with Algorithm 3 can be measured using the relative errors $\delta_{rel}\kappa$ and $\delta_{rel}n$, respectively. Note that all computations concerning the rod of the square cross section were performed with the C++ libraries for the floating-point conversions in the double extended precision format (dedicated for the Intel C++ compiler) as proposed in Jankowska (2010).

Consider the influence of the MFS and MPS parameters on the accuracy of the numerical solutions presented in Figs. 2–5. We can see that the smallest values of the relative errors $\delta_{rel}\kappa$ and $\delta_{rel}n$ for a given elastoplastic problem are obtained for c = 0.1, s = 0.2, *Ni* = 100 and d = 0.05 (*Nc* = 80) for both the lower and the upper range of $\tilde{\theta}$. Note that the accuracy is usually higher (except for the one presented in Fig. 4 and 5) and the number of Levenberg–Marquardt iterations lower, in the case of the lower range of $\tilde{\theta}$.

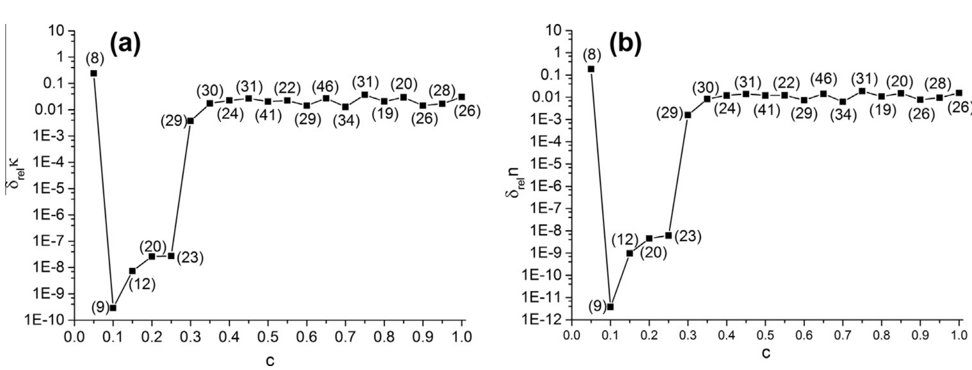

Fig. 7. The influence of the shape parameter c in the Kansa method on the accuracy of the approximate solution for the cylindrical cross section of the rod (N = 11, Ne = 21, κ_0 = 0.01, n_0 = 5.0).

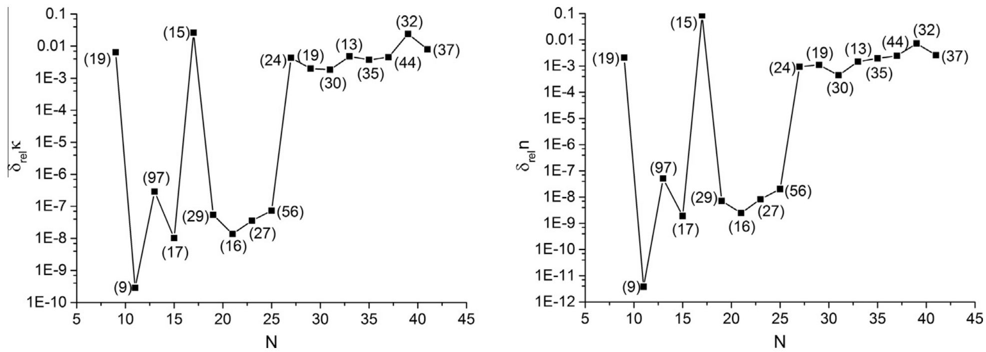

Fig. 8. The influence of the number of the nodes N in the Kansa method on the accuracy of the approximate solution for the cylindrical cross section of the rod ($Ne = 21$, $c = 0.1$, $\kappa_0 = 0.01$, $n_0 = 5$).

The higher accuracy is also possible if we use more data points in the Levenberg–Marquardt iteration procedure (see also Tables 1 and 2). In Tables 1 and 2 we consider the identification of the material parameters κ, n for different numbers Ne of data points and selected initial values κ_0, n_0 in the lower and the upper range of $\tilde{\theta}$, respectively. As we could expect, the greater number of Ne causes the increase of the numerical results accuracy with virtually constant number of iterations (more iterations is required only in the case of selected experiments in the upper range of $\tilde{\theta}$). Finally, we examine the influence of the random noise of data points on the accuracy of the identification process. As we can observe in Tables 3 and 4, the method proposed in the paper is stable and a small number of iterations is required. The higher accuracy can be observed for the greater number Ne of the data points used.

For the cylindrical cross section, all numerical experiments are performed for $N = 20$ nodes and $c = 0.2$. At the beginning, for four different pairs of coefficients κ, n, the direct problem for the circular cross section of the rod has been solved, and the results are shown in Fig. 6. The angle of twist per unit length $\tilde{\theta}$ in the range of 0.1–1.5, which determined the results of the torque $\tilde{M}_{T_i} = \tilde{M}_T(\tilde{\theta}_i)$, is similar for different pairs of $\{\kappa, n\}$. Therefore, when solving the inverse problem, the coefficients κ and n in the data $\{\tilde{M}_{T_i}, \tilde{\theta}_i\}_{i=1}^{Ne}$ are selected so that $\tilde{\theta}_i$ is in the range of [1.5, 3.0].

A numerical-experiment identification of the coefficients κ and n has been performed for different numbers of known pairs $\{\tilde{M}_{T_i}, \tilde{\theta}_i\}_{i=1}^{Ne}$ and various initial values of κ_0 and n_0. The input data $\{\tilde{M}_{T_i}, \tilde{\theta}_i\}$ have been generated by solving a direct problem (Algorithm 2) for given values of $\kappa = 0.023552997$ and $n = 3.83$ (chrome-nickel steel). The values of twist angles were determined using the formula $\tilde{\theta} = 1.5 + (i-1) \cdots 1.5/Ne$, where $Ne = \{15, 30, 45, 60\}$. Table 5 shows the results for five various pairs of the initial values $\{\kappa_0, n_0\}$ for the Levenberg–Marquardt method, i.e. $\{\kappa_0 = 0.0223725,\ n_0 = 3.6385\}$, $\{\kappa_0 = 0.1,\ n_0 = 3.447\}$, $\{\kappa_0 = 0.1,\ n_0 = 3.0\}$, $\{\kappa_0 = 0.01,\ n_0 = 4.0\}$ and $\{\kappa_0 = 0.01,\ n_0 = 5.0\}$. It can be observed that the convergence for the expected value of the identified parameters was not achieved in all examples. The convergence of the method affects both the initial value of κ_0, n_0 and the number of data Ne. Consider the influence of the Kansa method parameters on the accuracy of the numerical solutions presented in Figs. 7 and 8. We can see that the smallest values of the relative errors $\delta_{rel}\,\kappa$ and $\delta_{rel}\,n$ for a given elastoplastic problem are obtained for $c = 0.1$ (Fig. 7) and for $N = 11$ (Fig. 8). Table 6 shows the influence of the random noise of data of identification of the material parameters ($n = 3.83$, $\kappa = 0.023552997$) for $Ne = 21$ with, $\kappa_0 = 0.01$ and $n_0 = 5.0$. With the increase of noise of the data, identification of the material parameters deteriorates. However, the effect of random noise of data on the results of the identification is insignificant.

Table 6
The influence of the random noise of data points on the identification of the material parameters ($\kappa = 0.023552997$, $n = 3.83$) for a cylindrical cross section of the rod ($Ne = 21$, $N = 11$, $c = 0.15$, $\kappa_0 = 0.01$, $n_0 = 5.0$).

$\Delta\tilde{M}_T$ [%]	Iteration	κ	n	$\delta_{rel}\kappa$	$\delta_{rel}n$
0	12	0.023552997	3.83	7.44E−09	9.75E−10
0.25	8	0.023476408	3.83309867	3.25E−03	8.09E−04
0.5	6	0.023596855	3.83012018	1.86E−03	3.14E−05
0.75	4	0.023726488	3.81887235	7.37E−03	2.91E−03
1	7	0.021916546	3.87915112	6.95E−02	1.28E−02
1.25	7	0.023045787	3.84814142	2.15E−02	4.74E−03
1.5	6	0.02348428	3.83515395	2.92E−03	1.35E−03
1.75	6	0.023224161	3.88685395	1.40E−02	1.48E−02
2	3	0.023455756	3.9040352	4.13E−03	1.93E−02

5. Conclusions

A new inverse method to determine the elastoplastic properties of materials that were described by the Ramberg–Osgood stress–strain relation is proposed. In such stress–strain relation, there is an identical formula for the elastic and the elastoplastic regions, which permits an identical governing equation to be applied throughout the cross section. The algorithm is based on the knowledge of some couplings of the torsional moment and the angle of twist $\{\tilde{M}_{T_i}, \tilde{\theta}_i\}_{i=1}^{Ne}$, which allows one to obtain the non-dimensional material parameters κ and n in the Ramberg–Osgood's equation. In the proposed inverse method, the Leveberg-Marquadt iteration is used, which requires solving the direct problem at each iteration. The direct non-linear torsion problem is solved using Picard iteration procedure. For the prismatic cross section of the rod, at each iteration step, the method of fundamental solution and the method of particular solution are used. Particular solutions are obtained using the radial basis function. For the cylindrical cross section of the rod, the Kansa method is used at each iteration step. In both cases, the propose algorithms are easy to implement and can be used for complicated geometry because they are mesh-free. The Leveberg-Marquadt iteration method with the MFS (square rod) is always quickly convergent, and the Kansa method (circular rod) does not always guarantee a convergence to the expected results.

Acknowledgement

The paper has been supported by 21-381/2013 DS.

References

Baba, S., Kajita, T., 1982. Plastic analysis of torsion of a prismatic beam. Int. J. Numer. Methods Eng. 18, 927–944.

Baniassadi, M., Ghazavizadeh, A., Rahmani, R., Abrinia, K., 2010. A novel semi-inverse solution method for elastoplastic torsion of heat treated rods. Meccanica 45, 375–392.

Billinghurst, A., Williams, J.R.L., Chen, G., Trahair, N.S., 1992. Inelastic uniform torsion of steel members. Comput. Struct. 42, 887–894.

Bin-Mohsin, B., Lesnic, D., 2012. Determination of inner boundaries in modified Helmholtz inverse geometric problems using the method of fundamental solutions. Math. Comput. Simul.. http://dx.doi.org/10.1016/j.matcom.2012.02.002.

Chakrabarty, J., 1987. Theory of Plasticity. McGraw-Hill Book Company, New York.

Christopherson, D.G., 1940. A theoretical investigation of plastic torsion in an I-beam. J. Appl. Mech. 7, 1–4.

Dong, C.F., Sun, F.Y., Meng, B.Q., 2007. The method of fundamental solutions for inverse heat conduction problems in anisotropic medium. Eng. Anal. Bound. Elem. 31, 75–82.

Dwivedi, J.P., Upadhyay, P.C., Das Talukder, N.K., 1990. Torsional springback in square section bars of nonlinear wark-hardening materials. Int. J. Solids Struct. 32, 863–876.

Dwivedi, J.P., Upadhyay, P.C., Das Talukder, N.K., 1992a. Springback analysis of torsion of L-sectioned bars of work-hardening materials. Comput. Struct. 43, 815–822.

Dwivedi, J.P., Upadhyay, P.C., Das Talukder, N.K., 1992b. Parametric assessment of torsional springback in members of work-hardening materials. Comput. Struct. 45, 421–429.

Dwivedi, J.P., Shah, S.K., Upadhyay, P.C., Das Talukder, N.K., 2002. Sprimgback analysis of thin tectangular bars of non-linear wark-hardening materials under torsional loading. Int. J. Mech. Sci. 44, 1505–1519.

Hasanov, A., Tatar, S., 2010a. An inversion method for identification of elastoplastic properties of a beam from torsional experiment. Int. J. Nonlinear Mech. 45, 562–571.

Hasanov, A., Tatar, S., 2010b. Semi-analytic inversion method for determination of elastoplastic properties of power hardening materials from limited torsional experiment. Inverse Prob. Sci. Eng. 18, 265–278.

Hodge, P.G., 1966. A deformation bounding theorem for flow-law plasticity. Q. Appl. Math. 24, 171–174.

Hodge, P.G., 1967. Elastic–plastic torsion as a problem in non-linear programming. Int. J. Solids Struct. 3, 989–999.

Hodge, P.G., Herakovich, C.T., Stout, R.B., 1968. On numerical comparison in elasticplastic torsion. J. Appl. Mech. 35, 454–459.

Hon, Y.C., Wei, T., 2004. A fundamental solution method for inverse heat conduction problem. Eng. Anal. Bound. Elem. 28, 489–495.

Huth, J.H., 1955. A note on plastic torsion. J. Appl. Mech. 22, 432–434.

Jankowska M.A., 2010. Remarks on algorithms implemented in some C++ libraries for floating-point conversions and interval arithmetic. In: Lecture Notes in Computer Science vol. 6068 no.2, pp. 436–445. 8th International Conference on Parallel Processing and Applied Mathematics, PPAM 2009; Wroclaw; Poland.

Jin, B., Marin, L., 2007. The method of fundamental solutions for inverse source problems associated with the steady-state heat conduction. Int. J. Numer. Methods Eng. 69, 1570–1589.

Johansson, B.T., Lesnic, D., Reeve, T., 2011a. A comparative study on applying the method of fundamental solutions to the backward heat conduction problem. Math. Comput. Model. 54, 403–416.

Johansson, B.T., Lesnic, D., Reeve, T., 2011b. A method of fundamental solutions for the one-dimensional inverse Stefan problem. Appl. Math. Model. 35, 4367–4378.

Kansa, E.J., 1990. Multiquadrics – a scattered data approximation scheme with applications to computational fluid-dynamics – II solutions to parabolic, hyperbolic and elliptic partial differential equations. Comput. Math. Appl. 19, 147–161.

Karageorghis, A., Lesnic, D., 2011. Application of the MFS to inverse obstacle scattering problems. Eng. Anal. Bound. Elem. 35, 631–638.

Kliusznikov, W.D, 1979. Mathematical Theory of Plasticity. Moscow University, Moscow (in Russian).

Kołodziej, J.A., Gorzelańczyk, P., 2012. Application of the method of fundamental solutions for elasto-plastic torsion of prismatic rods. Eng. Anal. Bound. Elem. 36, 81–86.

Kołodziej, J.A., Mierzwiczak, M., Ciałkowski, M., 2010. Application of the method of fundamental solutions and radial basis functions for inverse heat source problem in case of steady-state. Int. Commun. Heat Mass 37, 121–124.

Lesnic, D., Bin-Mohsin, B., 2012. Inverse shape and surface heat transfer coefficient identification. J. Comput. Appl. Math. 236, 1876–1891.

Li, M., Chen, C.S., Hon, Y.C., 2011. A meshless method for solving nonhomogeneous Cauchy problems. Eng. Anal. Bound. Elem. 35, 499–506.

Mamedov, A., 1995. An inverse problem related to the determination of elastoplastic properties of a cylindrical bar. Int. J. Nonlinear Mech. 30, 23–32.

Mamedov, A., 1998. Determination of elastoplastic properties of a bimetallic and hollow bar. Int. J. Nonlinear Mech. 33, 385–392.

Marin, L., 2005. Numerical solution of the Cauchy problem for steady-state heat transfer in two-dimensional functionally graded materials. Int. J. Solids Struct. 42, 4338–4351.

Marin, L., 2011. Relaxation procedures for an iterative MFS algorithm for two-dimensional steady-state isotropic heat conduction Cauchy problems. Eng. Anal. Bound. Elem. 35, 415–429.

May, I.M., Al-Shaarbaf, I.A.S., 1989. Elasto-plastic analysis of torsion using a three-dimensional finite element model. Comput. Struct. 33, 667–678.

Mendelson, A., 1968. Plasticity: Theory and Application. MacMillan Company.

Mierzwiczak, M., Kołodziej, J.A., 2010. Application of the method of fundamental solutions and radial basis functions for inverse transient heat source problem. Comput. Phys. Commun. 181, 2035–2043.

Mierzwiczak, M., Kołodziej, J.A., 2011. The determination of heat sources in two dimensional inverse steady heat problems by means of the method of fundamental solutions. Inverse Prob. Sci. Eng. 19, 777–792.

Nadai, A., 1931. Plasticity. McGraw-Hill, New York.

Nadai, A., 1954. Theory of Flow and Fracture of Solids. McGraw-Hill, New York.

Press, W.H., Vetterling, W.T., Teukolsky, S.A., Flannet, B.P., 1992. Numerical Recipes in Fortran 77, second ed.. In: The Art of Scientific Computing. Cambridge University Press, New York, pp. 678–680 (Chapter 15).

Sadowsky, M.A., 1941. An extension of the sand heap analogy in plastic torsion applicable to cross-sections having one or more holes. J. Appl. Mech. 8, 166–168.

Shidfar, A., Darooghehgimofrad, Z., Garshasbi, M., 2009. Note on using radial basis functions and Tikhonov regularization method to solve an inverse heat conduction problem. Eng. Anal. Bound. Elem. 33, 1236–1238.

Shigeta, T., Young, D.L., 2009. The method of fundamental solutions with optimal regularization techniques for the Cauchy problem of the Laplace equation with singular points. J. Comput. Phys. 228, 1903–1915.

Smith, J.O., Sidebottom, O.M., 1965. Inelastic Behaviour of Load Carrying Members. John Wiley & Sons, New York.

Sokolovsky, V.V., 1942. On problem of elastic–plastic torsion. Prikl. Mat. Mekh. 6, 241–246 (in Russian).

Tsai, C.H., Young, D.L., Kolibal, J., 2011. Numerical solution of three-dimensional backward heat conduction problems by the time evolution method of fundamental solutions. Int. J. Heat Mass Transfer 54, 2446–2458.

Wei, T., Hon, Y.C., Ling, L., 2007. Method of fundamental solutions with regularization techniques for Cauchy problems of elliptic operators. Eng. Anal. Bound. Elem. 31, 373–385.

Wei, T., Chen, Y.G., Liu, J.C., 2013. A variational-type method of fundamental solutions for a Cauchy problem of Laplace's equation. Appl. Math. Model. 37, 1039–1053.

Xiong, X.T., Liu, X.H., Yan, Y.M., Guo, H.-B., 2010. A numerical method for identifying heat transfer coefficient. Appl. Math. Model. 34, 1930–1938.

Yamada, Y., Katagiri, S., Takatsuka, K., 1972. Elasto-plastic analysis of Saint-Venant torsion problem by a hybrid stress model. Int. J. Numer. Methods Eng. 5, 193–207.

Yan, L., Fu, C.L., Yang, F.L., 2008. The method of fundamental solutions for the inverse heat source problem. Eng. Anal. Bound. Elem. 32, 216–222.

Yan, L., Yang, F.L., Fu, C.L., 2009. A meshless method for solving an inverse spacewise-dependent heat source problem. J. Comput. Phys. 228, 123–136.

Yang, F.L., Ling, L., 2011. On numerical experiments for Cauchy problem for elliptic operators. Eng. Anal. Bound. Elem. 35, 879–882.

Yang, L., Yu, J.-N., Luo, G.-W., Deng, Z.-C., 2013. Numerical identification of source terms for a two dimensional heat conduction problem in polar coordinate system. Appl. Math. Model. 37, 939–957.

Zhou, D., Wei, T., 2008. The method of fundamental solutions for solving a Cauchy problem of Laplace's equation in multi-connected domain. Inverse Prob. Sci. Eng. 16, 389–411.